AIAA 81-0401R

Three-Dimensional Viscous Flowfield Computations in a Streamline Coordinate System

M.D. Kim,* R.R. Thareja,* and C.H. Lewis†
Virginia Polytechnic Institute and State University, Blacksburg, Va.

A method of predicting the three-dimensional laminar hypersonic viscous flowfield over a body at very high angles of attack has been developed by using the parabolized Navier-Stokes equations in a streamline coordinate system. At a very high angle of attack, the primary flow direction deviates substantially from the marching coordinate direction of the conventional body-generator coordinate direction. Hence, in the present approach the viscous flow equations are parabolized along the surface streamline direction instead of the body-generator coordinate direction, which reduces the restriction on the angle of attack of a flight vehicle. The streamline traces on the body surface are evaluated from a three-dimensional inviscid flowfield solution. Computational results for a test case have been obtained by both the present streamline approach (SLPNS) and the conventional body-generator coordinate method (PNS) for the purpose of comparison. The SLPNS results for the test case at moderate angle of attack compare well with conventional PNS results.

Nomenclature

CFS = streamwise skin-friction coefficient, $2\tau^*_{ws}/(\rho_\infty U^2_\infty)$
c_p = constant pressure specific heat
$ETA\,(=\eta)$ = normalized coordinate measured along ξ_2 coordinate, ξ^*_2/YSH^*
g = determinant of coordinate metric tensor
g_{ij} = coordinate metric tensor; $i,j=1,2,3$
g_1 = vector in the direction of ξ_1
g_2 = vector in the direction of ξ_2
g_3 = vector in the direction of ξ_3
H = total enthalpy, H^*/U^2_∞
h = static enthalpy, $h^*/c^*_pT_\infty$
M = freestream Mach number
p = pressure, $p^*/\rho_\infty U^2_\infty$
$\dot{q}$ = heat transfer, $\dot{q}^*/\rho_\infty U^3_\infty$
R^*_n = body nose radius of curvature
Re_∞/ft = freestream unit Reynolds number
$STINF$ = Stanton number, $\dot{q}^*/\rho_\infty U_\infty(H^*_0-H^*_w)$
s = surface distance coordinate measured along the body, s^*/R^*_n
T = temperature, T^*/T_∞
T_{ref} = reference temperature, $(\gamma-1)M^2_\infty T_\infty$ or U^2_∞/c^*_p
U_∞ = dimensional freestream velocity
u = velocity component along ξ_1 coordinate, u^*/U_∞
v = velocity component along ξ_2 coordinate, v^*/U_∞
V = local resultant velocity vector, V^*/U_∞
w = velocity component along ξ_3 coordinate, w^*/U_∞
X = equivalent cone slantwise length, X^*/R^*_n
YSH = shock-layer thickness, YSH^*/R^*_n
z,r,ϕ = body-oriented cylindrical coordinate system
α = angle of attack, deg
γ = ratio of specific heats
ϵ = perturbation parameter, $\epsilon^2=\mu^*(T_{\text{ref}})/\rho_\infty U_\infty R^*_n$
θ_c = cone half-angle, deg
μ = coefficient of viscosity, μ^*/μ_∞
ρ = density, ρ^*/ρ_∞
τ = shear stress
ξ_1 = streamline coordinate, streamwise direction
ξ_2 = streamline coordinate, body-normal and shock-normal direction
ξ_3 = streamline coordinate, normal to ξ_1 and ξ_2 on the body surface

Superscript

$(\,)^*$ = dimensional quantity

Subscripts

s = streamwise
w = wall value
0 = stagnation condition
∞ = freestream condition (dimensional quantity)

Introduction

In recent years the three-dimensional viscous shock-layer approach (VSL3D)[1] and the parabolized Navier-Stokes method (PNS)[2-4] have been applied to various problems for predicting hypersonic viscous flowfields over reentry vehicles. The viscous shock-layer equations (VSL3D) are parabolic in both streamwise and crossflow directions and are solved by efficient methods which require substantially less computing time than the PNS method. The VSL3D method can be applied to general geometries to obtain the flowfield solution over the entire body when the angle of attack is not too high. However, if the angle of attack becomes very large and a crossflow-separated region appears on the leeward side of the body, the method cannot treat that region. The PNS equations are parabolic in the streamwise direction and elliptic in the crossflow direction, which makes it possible to solve the crossflow separated region.

However, when the angle of attack becomes extremely high (e.g., over 45 deg), which often can be encountered during reentry flight, those two methods may not work even in the windward region of the vehicle for the following reason. Both conventional methods take the marching direction as the first coordinate direction of the body-generator coordinate system. But at very high angles of attack, the primary flow direction deviates substantially from the first body-generator coordinate direction, which may result in failure or very poor results in the flowfield solution.

Presented as Paper 81-0401 at the AIAA 19th Aerospace Sciences Meeting, St. Louis, Mo., Jan. 12-15, 1981; submitted March 6, 1981; revision received July 13, 1981.

*Graduate Student, Aerospace and Ocean Engineering Department. Student Member AIAA.
†Professor. Associate Fellow AIAA.

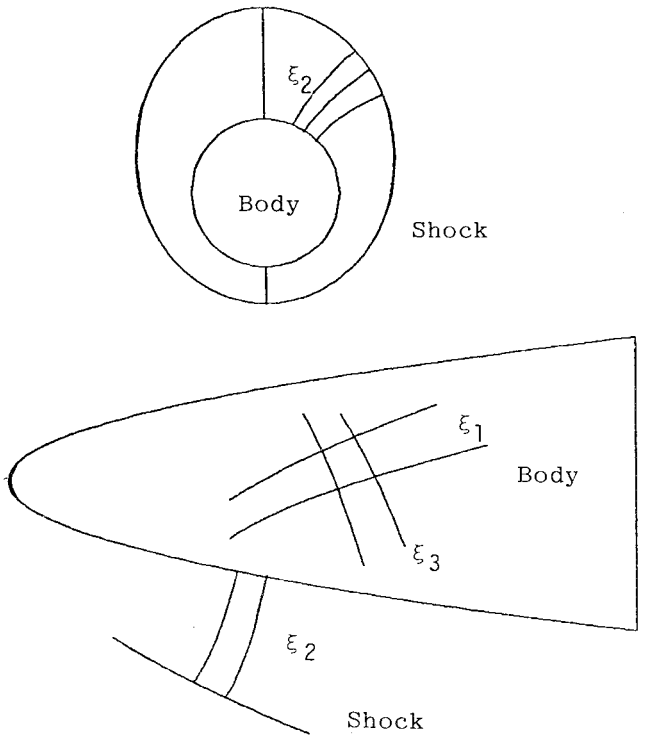

Fig. 1 Body-normal and shock-normal streamline coordinate system.

In the present approach (SLPNS), the same set of PNS equations are solved in a streamline coordinate system, which means that the governing equations are parabolized along the actual streamline direction, to be able to treat the cases of extremely high angle of attack. For the present analysis, the HYTAC code which has been developed by Helliwell et al.[5] is modified primarily in the parts related to the coordinate and metric generation.

A computational grid for the present flowfield analysis is generated numerically in a curvilinear streamline coordinate system. Streamline trace on the body surface constitutes the first coordinate (ξ_1), and it can be obtained by using an inviscid flowfield solution. In order to generate the third coordinate lines (ξ_3) to be normal to the streamlines on the body surface, an iterative numerical scheme has been developed. The second coordinate (ξ_2) is constructed by the procedure given by Helliwell,[4] which is body-normal, shock-normal, and always orthogonal to the ξ_1 and ξ_3 coordinates. Both SLPNS and PNS codes have been applied to a test case at a moderate angle of attack for the purpose of comparison.

Analysis

Generation of Streamlines on a Body Surface

The coordinate system for the present viscous flow analysis is a curvilinear streamline coordinate system as depicted in Fig. 1. The first coordinate (ξ_1) consists of surface streamlines, and the second coordinate (ξ_2) is body-normal and shock-normal. The third coordinate (ξ_3) is necessarily orthogonal to ξ_1 coordinate only at the body surface, while it is always orthogonal to the ξ_2 coordinate.

For the calculation of streamline traces on the body surface, an inviscid flowfield solution can be used. The inviscid flowfield can be obtained by using a set of three-dimensional inviscid flowfield programs developed by Marconi, Moretti, and co-workers[6-8] for general geometries, or by using another inviscid solver[9] for sphere-cone geometries. From the inviscid surface pressure and surface flow velocity distributions over a body, the streamline traces can be computed using the method developed by Hamilton.[10]

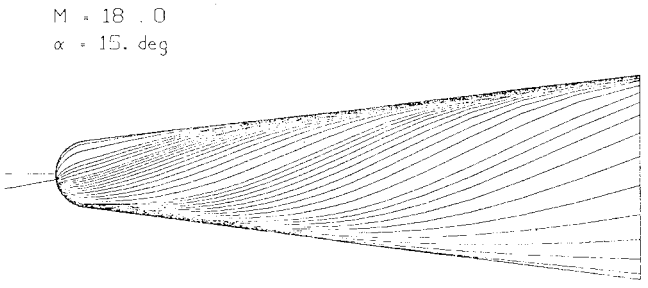

Fig. 2 Streamline trace on a sphere-cone.

In the nose region, the inviscid pressure distribution is used to find the direction of streamlines which start from the stagnation point on the spherical nose. In the case of a spherical nose, however, analytic streamlines also can be used. In the supersonic region which includes most of the body after the initial data plane, the three components of the inviscid velocity vector are used to determine the streamline direction on the body surface. With the surface streamline slopes known everywhere on the body surface, the surface streamline trace can be obtained by proper integration. A streamline pattern which has been obtained for the test case is shown in Fig. 2.

Computational Grid

The definition of a computational grid is one of the most crucial steps in building a numerical technique for a fluid-flow analysis. In the present study, surface streamlines constitute the first coordinate and the computational grid size is determined internally by the code, considering the number of iterations for a convergent solution. The inviscid streamlines need not be extremely accurate because the main purpose of the streamline coordinate system is to take the streamwise coordinate as the marching direction along which the governing equations are parabolized and, moreover, the equations for crossflow momentum are still taken into consideration.

The third coordinate lines (ξ_3) are constructed to be orthogonal to the ξ_1 coordinate lines on the body surface. Since the locations of streamlines are known, ξ_3 lines can be calculated by using the geometrical relationship of orthogonal lines and proper numerical iteration. From a given point on a ξ_1 line, a straight line segment is connected to the adjacent ξ_1 line. The desired grid point on the adjacent ξ_1 line can be obtained when this line segment has the same angle with ξ_1 lines at both ends. The desired grid point can be obtained by numerical iteration. After convergence of the iteration, the line segment becomes the chord of the corresponding ξ_3 coordinate line.

The second coordinate (ξ_2) is constructed to be normal to both ξ_1 and ξ_3 coordinate lines in the region between the body and the shock surface. This procedure is the same as the one which has been used by Helliwell et al.[4] in the HYTAC code. Since the shock surface is taken as a ξ_1,ξ_3 coordinate surface ($\xi_2=1$), the resulting ξ_2 coordinate lines will be both body-normal and shock-normal. In this coordinate system, the application of the shock boundary condition becomes simple because the ξ_2 coordinate is normal to the shock surface.

The reference coordinate system for the interpretation of the body geometry, the shock shape, and every computational grid point is a body-oriented cylindrical coordinate system, i.e.,

$$\xi_1=\xi_1(z,r,\phi) \tag{1}$$

$$\xi_2=\xi_2(z,r,\phi) \tag{2}$$

$$\xi_3=\xi_3(z,r,\phi) \tag{3}$$

When the computational grids are constructed in this manner, generally the ξ_1 and ξ_3 coordinates will not be orthogonal to each other in the region between the body and the shock. Hence the coordinate metric tensor g_{ij}, which is related to the nonorthogonality, will appear in the governing equations. In addition, the determinant of the metric g becomes an important factor in the governing equations. Figure 3 shows a ξ_1, ξ_3-grid shape on a developed cone which has been constructed numerically for the test case.

Governing Equations

In a general curvilinear coordinate system, the steady parabolized Navier-Stokes equations can be written in nondimensionalized form with the velocity vector written as

$$V = ug_1 + vg_2 + wg_3 \tag{4}$$

where u, v, and w are tensor velocity components. In the governing equations we will have the coordinate system metric tensor g_{ij}, which represents the coordinate stretching and nonorthogonality. In the equations for the stress tensor components, all the derivatives with respect to the primary streamline axis (ξ_1) were neglected. The resulting equations are parabolic in the ξ_1 axis direction and elliptic in the crossflow direction. The normal coordinate is normalized by the shock-layer thickness to facilitate the computation of the shock location. The complete set of the governing equations is given by Helliwell et al.[4]

The governing equations are solved by implicit differencing in the ξ_2,ξ_3 plane. The ξ_1 derivatives are approximated by a backward difference, while the ξ_2 and ξ_3 derivatives use an unequally spaced three-point difference scheme. After differencing, the equations are linearized by the Newton-Raphson method. The linearized equations are solved using the Gauss-Seidel iteration method. The details of the solution procedure for the equations can be found in Refs. 2-4.

Boundary Conditions

At the body, the no-slip conditions are used and enthalpy is specified. To obtain the pressure at the body surface, the v-momentum equation is used and two-point differencing in the body-normal direction is performed. At the plane of symmetry ($\phi = 0$ and 180 deg), w and g_{13} are antisymmetric, while all other flow variables and metrics are symmetric.

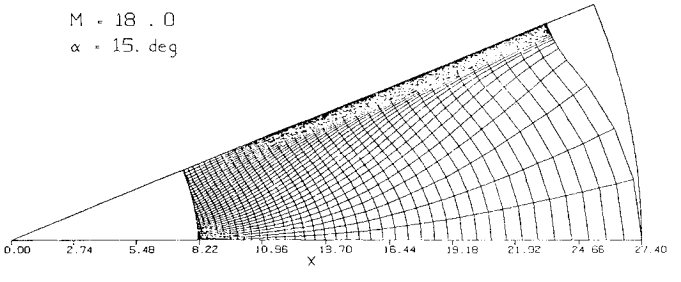

Fig. 3 $\xi_1\xi_3$ grid of a streamline coordinate system on a developed cone.

At the shock, the freestream velocity vector is transformed into the computational coordinate direction and then the Rankine-Hugoniot jump conditions are used. At this step, since the second computational coordinate $\xi_{12} \rightarrow \xi_2$ is normal to the shock surface, the conservation equations across the shock can be easily applied without further velocity vector rotations. Since the shock distance is also unknown, the continuity equation is used as a sixth equation, adding to the five conservation equations across the shock. The complete set of the equations for the boundary conditions can be found in Ref. 4.

Initial Data Plane

For a numerical flowfield solution which utilizes a marching scheme, the construction of an accurate initial data plane is one of the most crucial conditions for the success of the whole solution. In a previous investigation,[11] the viscous shock-layer method (VSL3D) for a blunt nose was found to be able to generate a satisfactory initial data plane to start the PNS solution. Thus, the entire flowfield including coordinates and metrics must be supplied at an initial data plane to get the SLPNS code started.

In the present study, it is noted that the streamline coordinate axes coincide with the wind axes on the spherical nose. Therefore, for the generation of an initial data plane in the streamline coordinate approach, the viscous shock-layer solution must be obtained only for the zero angle of attack regardless of the actual angle of attack concerned. At the initial data plane, the coordinate and metrics for the body-normal, shock-normal coordinate system are generated from the two step body-normal data of the viscous shock-layer solution by the method given by Helliwell et al.[4] The present method for initial data plane construction has a limit on angle of attack (maximum 45 deg) for two reasons. First, the initial data plane is constructed on the spherical nose portion using the axisymmetric viscous shock-layer solution. Second, the initial data plane must be in the supersonic flow region.

Finally, every grid point on the initial data plane which has been represented in a wind-oriented cylindrical coordinate system, must be represented in the body-oriented cylindrical coordinate system by a proper coordinate transformation because the reference coordinate system for the interpretation of the streamline coordinate system is the body-oriented cylindrical coordinate system.

Results and Discussion

As previously mentioned, the constructed streamline coordinate system has the following characteristics.

1) ξ_1 coordinate consists of the surface streamlines.
2) The body is a coordinate surface ($\xi_2 = 0$).

Table 1 Mach 18 test case freestream conditions

U_∞, ft/s (m/s)	T, °R (°K)	α, deg	θ_c, deg	Re_∞, ft^{-1} (m^{-1})	T_w/T_0	ϵ
7223 (2202)	62.8 (34.9)	15.0	7.0	544,700.0 (1,787,100.0)	0.127	0.055

Table 2 Test case computing times[a]

Method of solution	s from-to	s steps	Grid size of n points	ϕ planes	Time, min
SLPNS	1.31-7.11	31	50	19	3/6/27[b]
PNS	1.31-10.16	50	50	19	35.2

[a] CPU time on IBM 370/3032, H = OPT2 compiler.
[b] Inviscid solution/streamline solution/viscous solution.

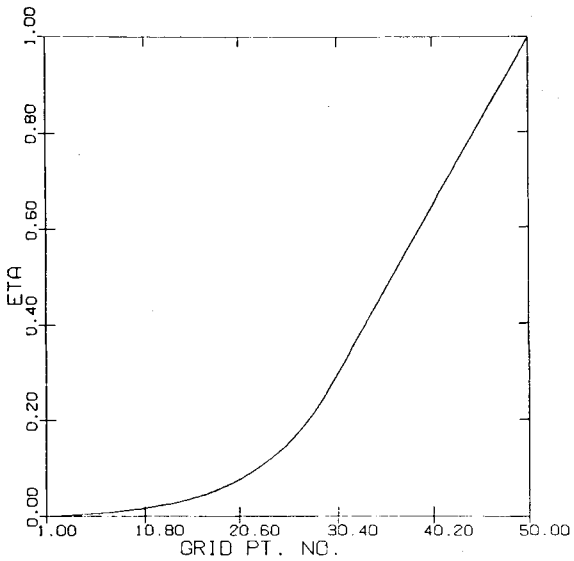

Fig. 4 Grid-point distribution normal to body surface.

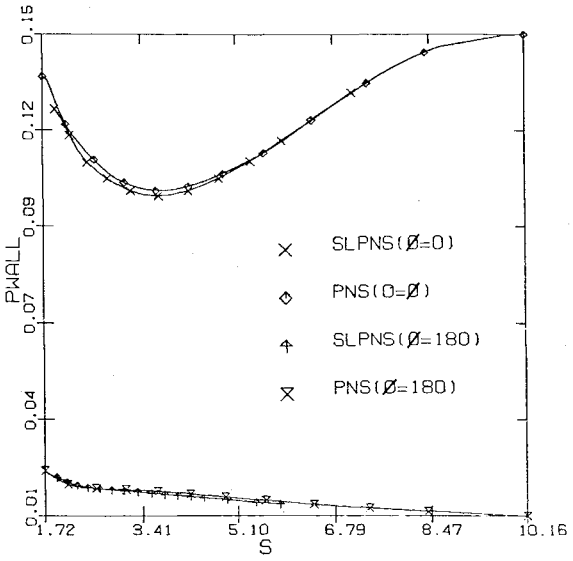

Fig. 7 Surface pressure distribution along the body.

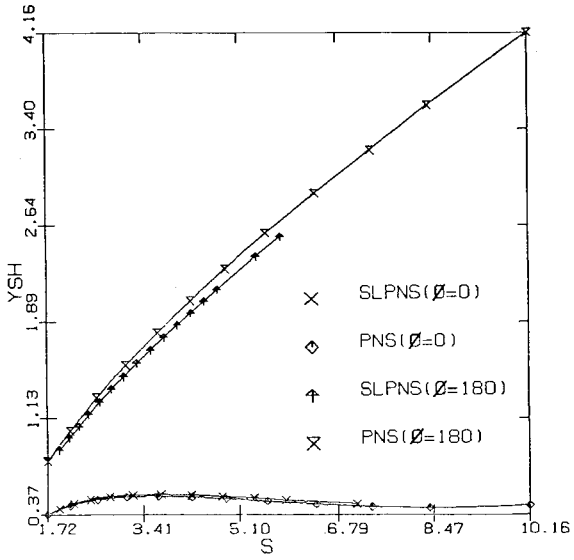

Fig. 5 Shock-layer thickness distribution along the body.

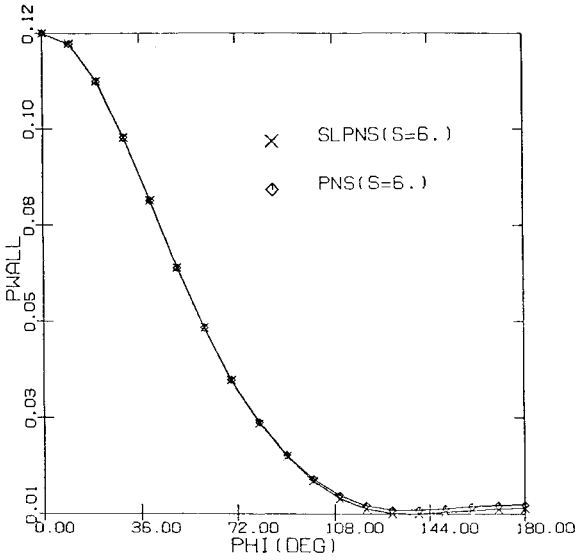

Fig. 8 Surface pressure distribution around the body.

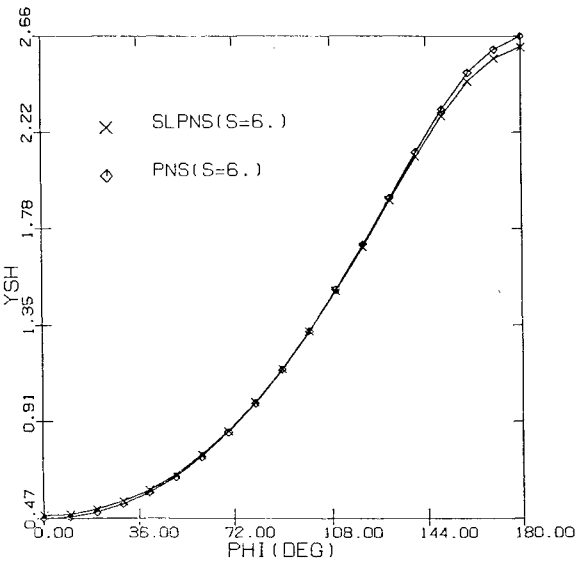

Fig. 6 Shock-layer thickness distribution around the body.

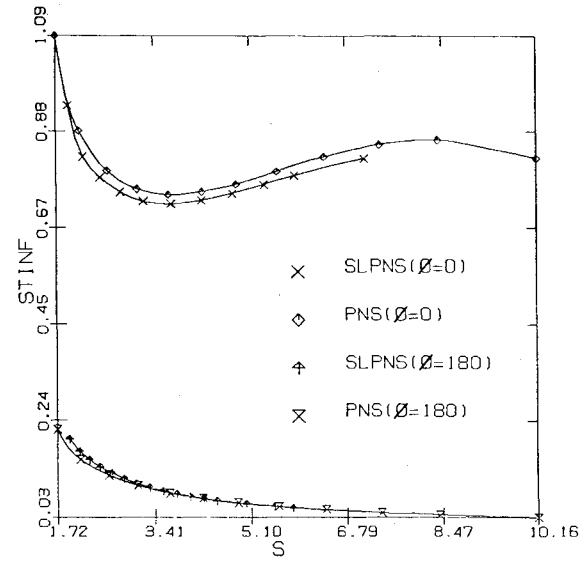

Fig. 9 Surface heat-transfer distribution along the body.

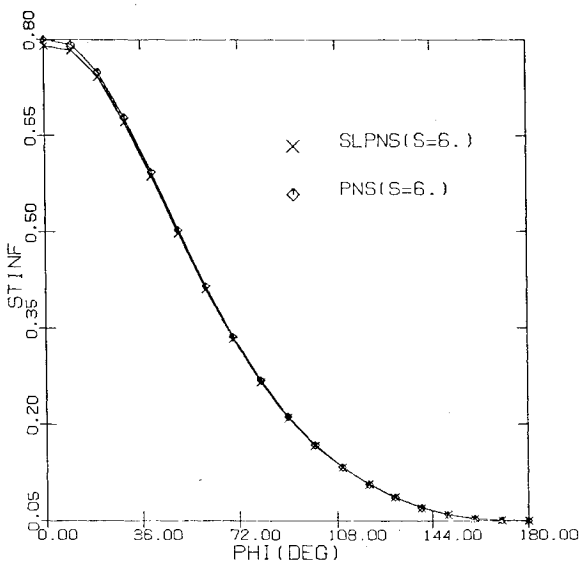

Fig. 10 Surface heat-transfer distribution around the body.

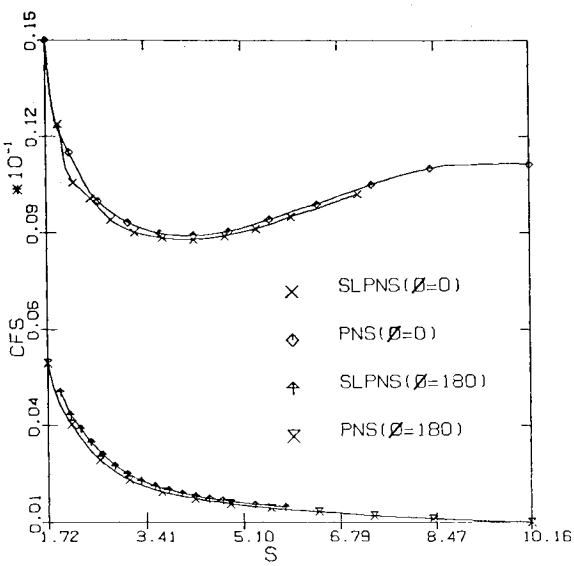

Fig. 11 Streamwise skin-friction distribution along the body.

3) The bow shock is a coordinate surface ($\xi_2 = 1$).

4) ξ_1 and ξ_3 coordinates are necessarily orthogonal only on the body surface.

5) ξ_2 coordinate is always orthogonal to ξ_1 and ξ_3 coordinates.

The shape of computed streamlines for the test case is presented in Fig. 2, and the numerically constructed ξ_1,ξ_3 grid on a developed cone is depicted in Fig. 3. The streamlines obtained from an inviscid flowfield in the spherical nose region were found to have slight deviations from the analytic solution. Hence, in the present work the analytic streamlines are used in the nose region. Moreover, the construction of the initial data plane becomes simpler when analytic streamlines are used in the nose region. The analytic streamlines in the nose region are linked with the numerical ones in the afterbody region by proper interpolations. Thus, the numerically constructed ξ_1,ξ_3 grid starts from the sphere-cone tangency point. Due to the slight discontinuity in the streamline slopes through the sphere-cone tangency point, the solution in that region took a relatively large number of iterations (10-13 times) and showed strong sensitivity to the marching stepsize. For the test cases it is observed that the streamlines on the windward side diverge rapidly from the neighboring streamlines, and the streamlines on the leeward side converge rapidly to the neighboring streamlines (see Fig. 3). Because of the rapid change in streamline pattern, the marching solution cannot be continued far downstream in a fixed streamline coordinate system.

For the purpose of demonstration, a test case at moderate angle of attack was chosen, and both SLPNS and PNS solutions were obtained. The results compare well with each other. The flow properties for the test case are shown in Table 1, and the computing times are presented in Table 2. It is observed that the two methods take similar computing times, and each method takes approximately 42 seconds per marching step on an IBM 370/3032 with OPT2 compiler. The normal grid distribution away from the body is shown in Fig. 4, where very small stepsizes were taken near the wall and nearly constant stepsizes away from the wall.

The computational results of shock-layer thickness, wall pressure, heat-transfer rate, and streamwise skin friction distributions for the test case are shown in Figs. 5-11. The slight differences between the two methods could have resulted from the different coordinate systems, the different initial plane data, and the different marching stepsizes. These results show that essentially identical results were produced for both methods at the modest angle of attack ($\alpha = 15$ deg).

With the satisfactory result in the streamline coordinate approach, it is also possible to use an artificially constructed quasistreamline coordinate if necessary, but the first coordinate direction should not deviate far from the streamwise direction.

Concluding Remarks

A procedure (SLPNS) has been developed to compute the viscous flowfield over general bodies at very high angles of attack by employing a streamline coordinate system. Comparisons with conventional PNS results for a test case indicate that the SLPNS method can accurately solve the flowfield in comparable computing time with the body-generator PNS method. SLPNS code itself can treat the cases of extremely high angles of attack (up to 90 deg), provided proper initial plane data and proper streamwise coordinate lines are supplied. Artificial streamwise coordinate lines also can be used when an inviscid streamline trace is not available or when it is required to obtain the solution far downstream on a long body. It is also possible to construct the coordinate system as one marches along the body by extrapolating streamline directions from the previous data plane at some level above the boundary layer and project these directions on to the body surface.

Acknowledgment

This research was supported by the Office of Naval Research under Contract N00014-79-C-0328.

References

[1] Murray, A.L. and Lewis, C.H., "Hypersonic Three-Dimensional Viscous Shock-Layer Flows over Blunt Bodies," *AIAA Journal,* Vol. 16, Dec. 1978, pp. 1279-1286.

[2] Lubard, S.C. and Helliwell, W.S., "Calculation of the Flow on a Cone at High Angle of Attack," *AIAA Journal,* Vol. 12, July 1974, pp. 965-974.

[3] Agopian, K., Collins, J., Helliwell, W.S., Lubard, S.C., and Swan, J., "NASA Viscous 3-D Flowfield Calculations," R&D Associates, RDA-TR-6100-007, Oct. 1975.

[4] Helliwell, W.S., Dickinson, R.P., and Lubard, S.C., "HYTAC Phase I Report, Viscous Flow over Arbitrary Geometries at High Angle of Attack," Areta Associates Technical Report, AR-79-046-TR, April 24, 1979.

[5] Helliwell, W.S., Dickinson, R.P., and Lubard, S.C., "HYTAC User's Manual," Arete Associates Technical Report, AR-80-207-TR, July 31, 1980.

[6] Marconi, F., Salas, M., and Yaeger, L., "Development of a Computer Code for Calculating the Steady Super/Hypersonic Inviscid Flow around Real Configurations," Vol. I—Computational Technique, NASA-CR-2675; Vol. II—Code Description, NASA-CR-2676, April 1976.

[7]Marconi, F., Yaeger, L., and Hamilton, H.H., "Computation of High Speed Inviscid Flow about Real Configurations," *Proceedings of Conference on Aerodynamic Analysis Requiring Advanced Computers,* Part II, NASA-SP-347, March 1975.

[8]Moretti, C. and Bleich, G., "Three-Dimensional Flow Around Blunt Bodies," *AIAA Journal,* Vol. 5, Sept. 1967, pp. 1557-1562.

[9]Solomon, J.M., Ciment, M., Ferguson, R.E., Bell, J.B., and Wardlaw, A.B. Jr., "A Program for Computing Steady Inviscid Three-Dimensional Supersonic Flow on Reentry Vehicles, Vol. 1, Analysis and Programming," Naval Surface Weapons Center, NSWC-WOL-TR-7728, Feb. 1977.

[10]Hamilton, H.H. II, "Calculation of Heating Rates on Three-Dimensional Configurations," Thesis for Degree of Engineer, School of Engineering and Applied Science of the George Washington University, Dec. 1979.

[11]Waskiewicz, J.D. and Lewis, C.H., "Hypersonic Viscous Flows over Sphere-Cones at High Angles of Attack," AIAA Paper 78-64, Jan. 1978.

[12]Srivastava, B.N., Werle, M.J., and Davis, R.T., "Viscous Shock-Layer Solutions for Hypersonic Sphere-Cones," AIAA Paper 77-693, June 1977.